Chem. Chem. Technol., 2022,
Vol. 16, No. 4, pp. 581–590

Chemistry

NUCLEOTIDE INTERACTION WITH NANOCRYSTALLINE CERIA SURFACE

***Nataliia Vlasova*[1, ✉], *Olga Markitan*[1]**

https://doi.org/10.23939/chcht16.04.581

Abstract. The adsorption of nucleotides on the surface of nanocrystalline cerium dioxide (pH_{pzc} = 6.3) in NaCl solutions was investigated using multi-batch adsorption experiments over a wide range of pH. The obtained results were interpreted as a formation of outer and inner sphere surface complexes with the participation of phosphate moieties. The Basic Stern surface complexation model was applied to obtain quantitative equilibrium reaction constants.

Keywords: ceria**,** nucleotide, adsorption, surface complexation theory.

1. Introduction

The interface between biomolecules and inorganic oxide surfaces has attracted considerable attention as a decisive factor in the bio-applications of nanostructured oxides.[1-6] One of the important inorganic oxides with unique properties is the nanosized cerium dioxide. Cerium oxide nanoparticles have received much attention because of their excellent catalytic activities, which are derived from the change of the oxidation state between Ce^{+4} and Ce^{+3}. Being a mature engineered nanoparticle with various industrial applications, the nanoparticles of CeO_2 were recently found to have multi-enzyme (including superoxide oxidase, catalase, and oxidase) and mimetic properties, which produce various biological effects. They are potential antioxidants towards almost all noxious intracellular reactive oxygen species.[7,8] Cerium dioxide has emerged as a fascinating and lucrative material in biological fields such as bioanalysis,[9-11] biomedicine,[12] drug delivery,[13,14] and bioscaffolding.[15,16]

Deoxyribonucleic acid (DNA) has recently become an important molecule in bionanotechnology and is widely used in biosensing, medical diagnostics, and imaging.[17-19] It is also widely used in a variety of nanomaterial modifications[20,21] due to its special structure and properties. The interaction between DNA and nanoceria draws much attention.[21-23]

For all these applications understanding of the interaction at a nano-bio interface plays a key role in the development of nanoscience and nanotechnology.

Defining the interaction of oxide particles with biopolymers is an extremely complex task. Such interactions are very complicated because they include the formation of many different in-nature bonds involving numerous groups of biomolecules and surface functional groups of the solid[3,5,6,24] Studies of the interaction of nanooxide surface with monomeric biomolecules such as nucleotides, from which the corresponding biopolymers – nucleic acids, are formed, can serve as a basis for establishing the mechanism at the molecular level.

The aim of this paper is to study the nucleotides adsorption at the ceria/aqueous solution interface in terms of surface complexation theory. This approach allows to quantitatively determine the stability of surface complexes and to predict the types of interaction between adsorbable molecules and active sites of solid.

2. Experimental

A nanocrystalline cerium dioxide (nanopowder, Aldrich) with a specific surface area of 60 ± 5 m^2/g (Nova 1200, Quantachrome) was used. According to X-ray diffraction data (Dron-3M diffractometer), cerium dioxide has a cubic fluorite structure. The crystallite size calculated by the Sherrer equation is 30 nm, which corresponds to the manufacturer's data (<25 nm).

2.1. Potentiometric titration

Potentiometric titration of ceria suspension (5 g/L) with acid and base was performed at 298 K in a thermostated reactor (50 mL) with a magnetic stirrer and a tube for bubbling with Ar. The ionic strength was adjusted by a background electrolyte to 0.01 and 0.1 M using NaCl (Merck, p.a.). The pH of the suspension was measured using the Inolab Level 2P pH meter (WTW) equipped with a combined electrode (SenTix81) and temperature probe. The electrode was calibrated using 3-point

[1] Chuiko Institute of Surface Chemistry of the National Academy of Sciences of Ukraine
17, Generala Naumova St., Kyiv, 03164, Ukraine
✉ *natalie.vlasova@gmail.com*

calibration with a commercial pH buffer (CertiPure, Merck) to a precision of ±0.02 units. The titrations were carried out in batch mode by discrete additions of dilute HCl or NaOH prepared from standard solutions (Titrisol, Merck) in deionized water under bubbling with Ar. Electrode readings were taken, when a drift less than 0.002 pH units in 10 min was attained, with a minimum reading time of 15–20 min between additions.

2.2. Sorption experiments

For adsorption experiments, nucleotides (all from Reanal, p.a.) were used as received: pyrimidine nucleotides as a sodium salt of cytidine-5'-monophosphate, uridine-5'-monophosphate, and purine nucleotides as sodium salts of adenosine-5'-monophosphate, guanosine-5'-monophosphate.

The nucleotide adsorption was studied at 293 K. Equal volumes of ceria suspension (2 g/L) and nucleotide solutions (0.2 mmol/L) were mixed in centrifuge tubes. A constant ionic strength (0.01 M) was maintained by the addition of background electrolyte NaCl. The pH value was adjusted to the desired value between 2 and 9 with HCl or NaOH solutions. All suspensions were stirred for 2 h, a final pH was measured, and then the solid phase was separated by centrifugation (8000 rpm, 20 min). It was preliminary found that the time of 2 h was sufficient to reach the adsorption equilibrium. Nucleotide concentrations were determined from the absorption spectra in the UV region (Specord M-40 spectrophotometer, Carl Zeiss Jena). They are characterized by absorption bands at 260-270 nm. The dependences of position and intensity of the bands on pH values were determined before.

The amounts of adsorbed nucleotides (in μmol/g) were calculated as the difference between initial and equilibrium concentrations. Experimental adsorption values are shown in the Figures as symbols, and the calculated adsorption curves are shown as lines.

2.3. Model calculations

The Basic Stern surface complexation model[25,26] and the GRFIT software[27] are used for quantitative interpretation of experimental data. The GRFIT program is very convenient because the fitting of adjustable parameters is accompanied by a graphic drawing of an adsorption curve, revealing if the choice of reaction equations and initial values of the adjustable parameters was successful. The first step of the work is the choice of the solution components, solid components, and charges in different planes of the interface. The solution components are initial species of biomolecule, proton, and electrolyte ions. The initial hydroxyl group (≡CeOH) and electrical components exp0 and exp1 are considered to be surface components. Electrical components corresponding to the charge values of the species in the 0 and 1 planes of the interface. They are expressed as coefficients of the potentials at the respective planes of the electric double layer (EDL). The next step is to create a matrix in which the species in the solution (all other forms of dissolved substances than initial ones) and surface species (protonated and an ionized surface hydroxyl group), ion-pairs with background electrolyte ions, and surface complexes with nucleotides are defined as combinations of components.

It should be also noted that the program requires knowledge of such solid characteristics as the specific surface area and concentration of functional groups or site density. The concentration of functional groups can be set as an adjustable parameter or is selected based on data, for example, acid-base titration of the oxide suspension.

3. Results and Discussion

3.1. Acid-base properties of ceria surface groups

The charging of oxide surfaces due to the interaction with protons of aqueous solution results in the formation of an electrical double layer between an electrolyte solution and oxide surface, which affects the complexation reactions with inorganic and organic molecules. Surface complexation theory was successfully used to describe the binding of protons by active groups of oxide surfaces.[28] The acid-base properties of the surface groups of the oxide are always investigated before studying the adsorption interactions of chemical compounds.

The potentiometric titration data on ceria suspensions were used to calculate the surface charge depending on pH and ionic strength (Fig. 1). These data indicate that the curves are intersected at the point of zero charges (PZC) at pH 6.3. The PZC values reported in the literature for cerium dioxide vary within a rather broad range of 5.2–8.2. Such a broad range of PZC values can probably be explained by the fact that the studied cerium dioxide samples were synthesized by different methods and had different particle sizes.[29]

The Basic Stern complexation model was used to quantitatively estimate the protolytic properties of cerium dioxide and adsorption equilibria with organic molecules. According to this model, an interface consists of two planes. Potential determining ions are adsorbed in one of them (plane or layer 0), whereas weakly bound counterions are adsorbed in another plane, the internal Helmholtz plane, which is denoted as a plane or layer 1 (Fig. 2).

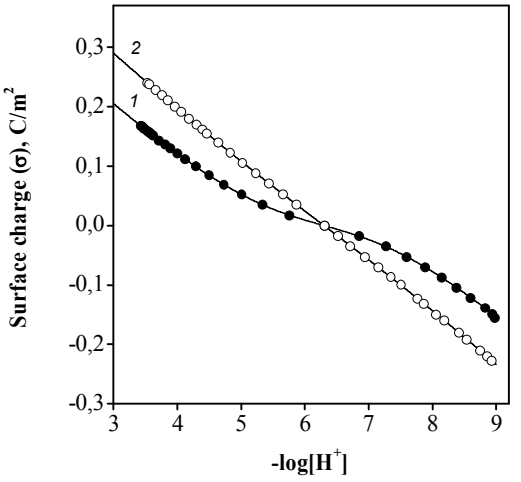

Fig. 1. Experimental (symbols) surface charge values of ceria and those calculated using Basic Stern model (solid line) as the function of pH and ionic strength: C_{oxide} = 5 g/L, and C_{NaCl} = 0.01 (*1*) and 0.1 M (*2*)

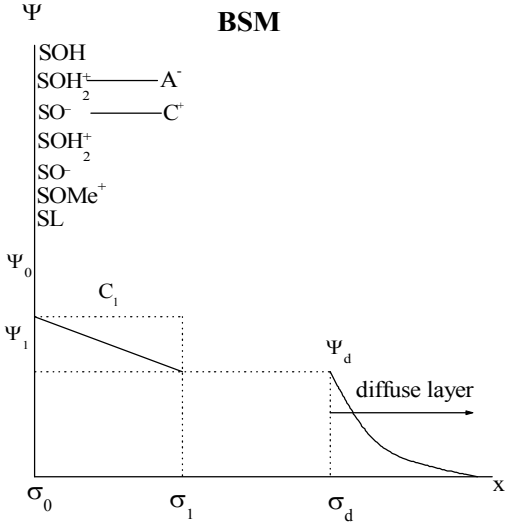

Fig. 2. The structure of double electric layer (Basic Stern model) at ceria/aqueous electrolyte solution interface: Ψ is the potential; σ is the surface charge; symbols of charges of σ_0 and σ_1 correspond to planes 0 and 1, respectively

The results of potentiometric titration of ceria suspensions were used to calculate surface charge σ_0 (C/m^2) by the following equation:

$$\sigma_0 = (F / SC_{oxide})(C_A - [H^+] - C_B + [OH^-]), \qquad (1)$$

where F is the Faraday constant (96485 C/mol); S is the specific surface area (m^2/g); C_{oxide} is the concentration of ceria (g/L) taken for titration; C_A and C_B are concentrations of added acid and base (mol/L), [H$^+$] and [OH$^-$] are equilibrium concentrations of protons and hydroxyls recalculated from activities measured by pH-meter.

According to the surface complexation theory, surface hydroxyl groups are considered to be amphoteric ones, and the interaction between functional groups and protons of an aqueous solution leads to either protonation or ionization of these groups:

$$\equiv CeOH + H^+ \leftrightarrow \equiv CeOH_2^+$$
$$\equiv CeOH \leftrightarrow \equiv CeO^- + H^+$$

These protolytic equilibria are characterized by corresponding constants:

$$K_{S1}^{int} = \frac{[CeOH_2^+]}{[CeOH][H^+]} \exp(F\Psi_0 / RT),$$
$$\log K_{S1}^{int} = 4.73 \pm 0.05$$
$$K_{S2}^{int} = \frac{[CeO^-][H^+]}{[CeOH]} \exp(-F\Psi_0 / RT),$$
$$\log K_{S2}^{int} = -7.87 \pm 0.05,$$

where [CeOH], [CeOH$_2^+$], and [CeO$^-$] are the equilibrium concentrations of neutral, protonated, and ionized surface hydroxyl groups (mol/L), Ψ_0 – oxide surface potential on 0-plane, T – temperature, K.

Background electrolyte ions interact with surface hydroxyl groups to form ion-pair type complexes or so-called outer-sphere complexes.[25,28] Hence, to describe the protolytic properties of the oxide, the formation reactions of outer-sphere complexes with electrolyte ions must be taken into account, in addition to the protonation and ionization reactions:

$$\equiv CeOH + H^+ + A^- \leftrightarrow \equiv CeOH_2^+ A^-$$
$$\equiv CeOH + C^+ \leftrightarrow \equiv CeO^- C^+ + H^+$$

The equilibria of these reactions are described by corresponding constants:

$$K_A^{int} = \frac{[CeOH_2^+ A^-]}{[CeOH][H^+][A^-]} \exp F(\Psi_0 - \Psi_1)/RT,$$
$$\log K_A^{int} = 5.73 \pm 0.05$$

$$K_C^{int} = \frac{[CeO^- C^+][H^+]}{[CeOH][C^+]} \exp F(\Psi_1 - \Psi_0)/RT,$$
$$\log K_C^{int} = -6.87 \pm 0.05,$$

where Ψ_1 is oxide surface potential in plane 1; C$^+$ and A$^-$ correspond to the cation and anion of background electrolyte.

Taking into account all reactions proceeded on the ceria surface in the presence of aqueous electrolyte solution, the surface charge density may be expressed by the following equation:

$$\sigma_0 = (F / SC_{oxide})([CeOH_2^+] + [CeOH_2^+ A^-] - [CeO^-] - [CeO^- C^+]).$$

Thus, the equilibrium reaction constants of protonation–ionization and ion-pair formation reactions

were determined by comparing the surface charge values calculated by Eq. (1) and the values selected by GRFIT software using the method of successive approximations. The best agreement between experimental data and calculated curves was achieved for the set of parameters presented directly next to constant expressions.

3.2. Nucleotides' adsorption

The reaction of nucleotides and cerium dioxide functional groups were interpreted as the formation of adsorption complexes. These complexes may involve nucleotides with different degrees of protonation and hydroxyl groups of the adsorbent.

Nucleotide, which is the main repeating unit of nucleic acid molecules, is a phosphorylated nucleoside. A nucleoside consists of bases (purine and pyrimidine ones), which are bonded by β-glycoside bonds with carbohydrate units. Carbohydrate residue replaces a hydrogen atom at the N-1 nitrogen atom of pyrimidine base or N-9 of purine one.

Heterocyclic bases, which are contained in nucleotides, significantly differ in the basicity of nitrogen atoms. The protonation of active base sites in adenosine-5'-monophosphate and cytidine-5'-monophosphate is observed at pH < 4, and, in the case of guanosine-5'-monophosphate, it is seen at pH < 2.3. In the studied pH range, the heterocyclic uridine-5'-monophosphate base is neutral.[30,31] Primary ionization of the phosphate groups in nucleoside monophosphates (NMPs) occurs at pH < 2, while ionization of secondary groups is observed at pH > 6.1.[31,32] Table 1 summarizes the formulas and ionization constants of the studied NMPs. Fig. 3 shows the solution speciation for different forms of studied nucleotides: nucleotides can be present in solutions as zwitterion ($H_2L^{\pm}$), monoanion (HL^{-}), and dianion (L^{2-}) depending on pH.

Table 1. Nucleotides and their ionization constants[31]

Formula, name	Ionization constants, pK_n (0.01 M)
purine	
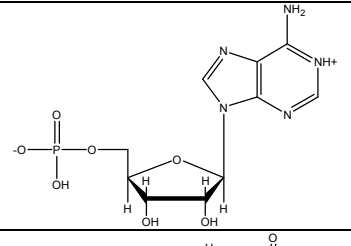 adenosine-5'-monophosphate (AMP)	3.83 (N_1–H^+) 6.46 (–PO_3H^-)
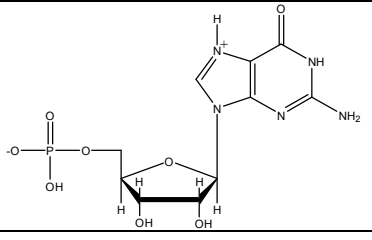 guanosine-5'-monophosphate (GMP)	2.47 (–N_7H^+) 6.48 (–PO_3H^-)
pyrimidine	
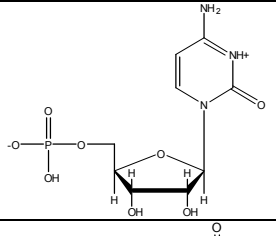 cytidine-5'-monophosphate (CMP)	4.31 (N_3–H^+) 6.15 (–PO_3H^-)
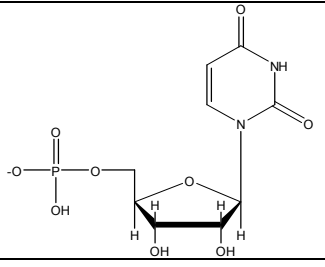 uridine-5'-monophosphate (UMP)	6.04 (–PO_3H^-)

The dependence of nucleotides adsorption on pH values is shown in Fig. 4. To determine possible adsorption reactions, the state of oxide surface groups and the forms, in which nucleotides occur in the solution, should be found as a function of pH. Regarding the functional groups of ceria, hydroxyl groups are protonated in an acidic medium, while ionized groups prevail at pH values above the point of zero charges. An increase in the NMP adsorption is observed at pH values, which approximately correspond to the deprotonation constant of the nitrogen atoms of nucleic bases. At pH > 6, the adsorption decreases due to the repulsion of similarly charged anions and ionized surface groups of oxide. Thus, it has been established that stable complexes are formed on the ceria surface due to the electrostatic interactions between the protonated surface groups and anionic forms of nucleotides resulting from the ionization of phosphate residues.

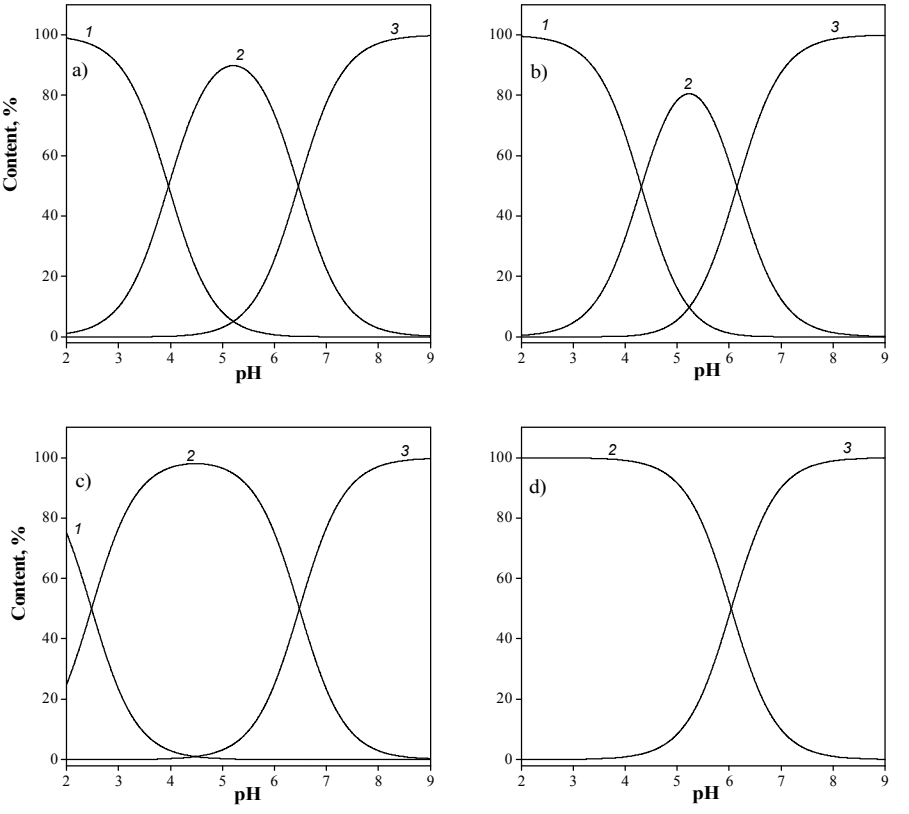

Fig. 3. Distribution diagrams for AMP (a), CMP (b), GMP (c), and UMP (d): zwitter ion $H_2L^{\pm}$ (*1*), monoanion HL^{-} (*2*), and dianion L^{2-} (*3*)

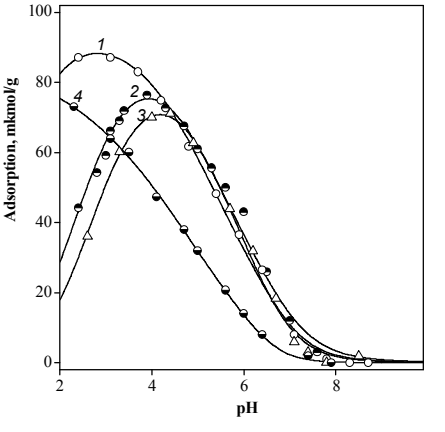

Fig. 4. Adsorption of GMP (*1*), AMP (*2*), CMP (*3*), and UMP (*4*) on the ceria surface as a function of pH: C_{NMP} = 0.1 mmol/L, C_{oxide} = 1 g/L, 0.01 M NaCl. Experimental and calculated data are shown by symbols and curves, respectively

Table 2. Complex formation reactions and corresponding equilibrium reaction constants (logK ± 0.05)

	Surface reaction	Equilibrium reaction constant	AMP	GMP	CMP	**UMP**
Equilibrium surface reaction constants of complex formation						
1	$\equiv CeOH + H_2L^{\pm} \leftrightarrow \equiv CeOH_2^+ HL^-$	$K = \frac{[CeOH_2^+ HL^-]}{[CeOH][H_2L^{\pm}]} \exp(F(\Psi_0 - \Psi_1)/RT)$	5.18	6.52	4.88	
2	$\equiv CeOH + H_2L^{\pm} \leftrightarrow \equiv CeOH_2^+ L^{2-} + H^+$	$K = \frac{[CeOH_2^+ L^{2-}][H^+]}{[CeOH][H_2L^{\pm}]} \exp(F(\Psi_0 - 2\Psi_1)/RT$	-0.67	0.55	-1.04	
3	$\equiv CeOH + HL^- + H^+ \leftrightarrow \equiv CeOH_2^+ HL^-$	$K = \frac{[CeOH_2^+ HL^-]}{[CeOH][HL^-][H^+]} \exp(F(\Psi_0 - \Psi_1)/RT$				8.19
4	$\equiv CeOH + HL^- \leftrightarrow \equiv CeOH_2^+ L^{2-}$	$K = \frac{[CeOH_2^+ L^{2-}]}{[CeOH][HL^-]} \exp(F(\Psi_0 - 2\Psi_1)/RT$				2.51
Stability constants of surface complexes						
5	$\equiv CeOH_2^+ + HL^- \leftrightarrow \equiv CeOH_2^+ HL^-$	$K = \frac{[CeOH_2^+ HL^-]}{[CeOH_2^+][HL^-]} \exp(F(\Psi_0 - \Psi_1)/RT$	4.42	4.28	4.47	3.47
6	$\equiv CeOH_2^+ + L^{2-} \leftrightarrow \equiv CeOH_2^+ L^{2-}$	$K = \frac{[CeOH_2^+ L^{2-}]}{[CeOH_2^+][L^2]} \exp(F(\Psi_0 - 2\Psi_1)/RT$	5.00	4.79	4.70	3.83
7	$\equiv CeOH + HL^- \leftrightarrow \equiv CeOL^- + H_2O$	$K = \frac{[CeOL^-]}{[CeOH][HL^-]} \exp(F(-\Psi_0)/RT$	3.23	3.07	3.23	2.25

Based on a comparison of the nucleotide forms in the solution and the state of the surface functional groups, the possible reactions of complexes formation were chosen. Table 2 shows the reaction equations and expressions of the corresponding equilibrium constants, obtained for the best agreement between the experimental and calculated values of adsorption.

The reactions (1) – (4) listed in Table 2 lead to the formation of electrostatic or outer-sphere complexes due to the interaction between positively charged protonated groups and negatively charged nucleotide anions. The distribution diagrams of nucleotide adsorption complexes on the ceria surface (Fig. 5) depending on pH were plotted based on the calculated equilibrium reaction constants. It should be noted that curves corresponding to different complexes intersect at pH – 6. This value correlates with the ionization constant of singly charged anion, *i.e.*, ionization of monoanion adsorbed on the surface and in the solution occurs at the same pH value.

All calculated equilibrium reaction constants may be converted into stability constants of complexes taking into account the protonation of CeOH groups and protonation/ionization of nucleotides. The stability constants of surface complexes represented in Table 2 (reactions 5, 6) are more convenient to be compared with each other.

The more stable complexes form nucleotides, the heterocyclic bases of which are capable of protonation, *i.e.*, AMP, CMP, and GMP. The stability constants of complexes with a singly charged anion are somewhat lower than those of complexes with a doubly charged anion. A similar regularity is also observed for the complexes of some transition metals with inorganic phosphates.[33,34] This analogy is possible because we assume the binding of the nucleotide anions to the surface via phosphate groups. It was interesting to compare adsorptions of nucleotides (organic phosphates) and inorganic orthophosphate (OP) and corresponding equilibrium reaction constants. The pH dependence of orthophosphate was studied under the same experimental conditions as for nucleotides (Fig. 6).

To select possible complexation reaction in case of the orthophosphate adsorption, we took into account protolytic properties of tribasic orthophosphoric acid: $pK_1 = 2.06$, $pK_2 = 7.02$ and $pK_3 = 12.1$.[35] The adsorption values of OP slightly decrease with increasing pH, which can be explained by the binding of phosphate anions with a protonated ceria surface and the formation of electrostatic outer-sphere complexes. The adsorption curve simulation (GRFIT) shows the best conformity for the formation of only one complex with doubly charged anion $\equiv CeOH_2^+ HL^{2-}$, the stability constant of which is $\log K_{HL}^{int} = 7.84 \pm 0.05$.

Comparison of the adsorption curves of phosphate and nucleotides shows that the nature of the heterocyclic base affects the curve form.

According to the literature data,[36-41] phosphate adsorption on the surfaces of titanium and iron oxides is interpreted as the formation of covalently bound complexes, although the available spectroscopic data do not give an unambiguous answer about the type of bonds in these complexes. If we assume the formation of inner-sphere phosphate complexes on the surface of cerium dioxide, the adsorption curves must be simulated taking into account the following reactions:

$$\equiv CeOH + HO(P{=}O)(OH)_2 \leftrightarrow$$
$$\leftrightarrow \equiv CeO(P{=}O)(OH)_2 + H_2O, \quad (2)$$

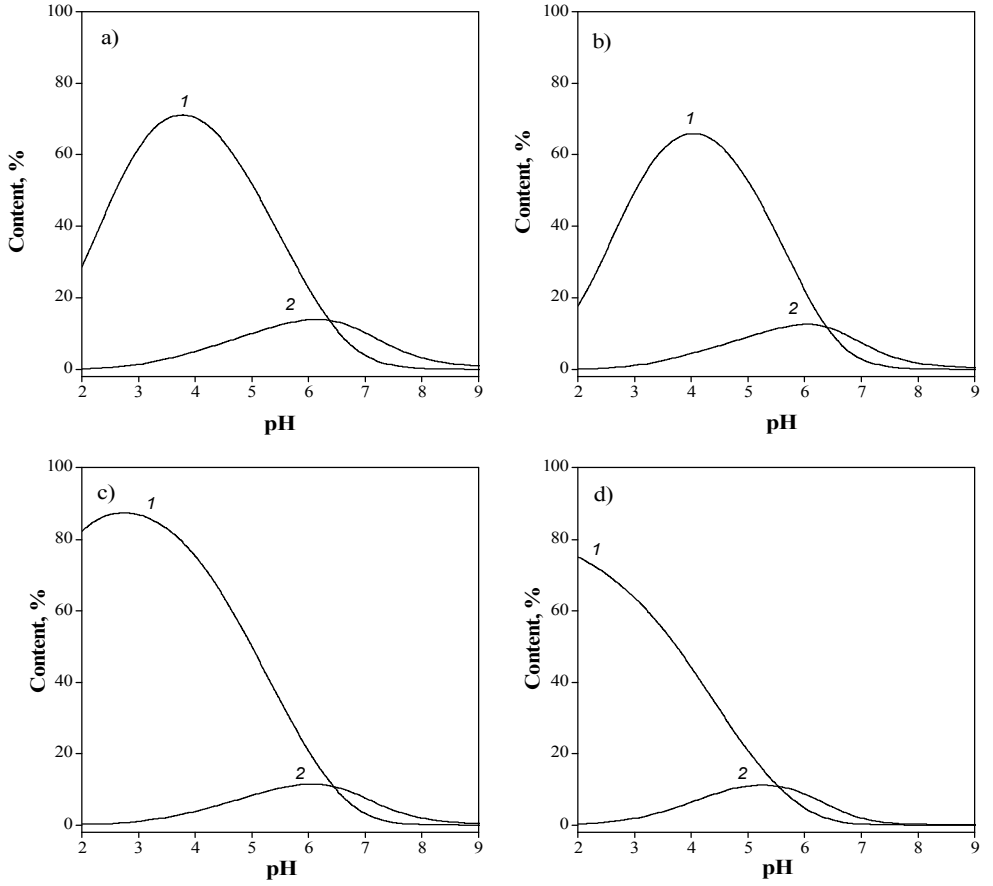

Fig. 5. Surface speciation of adsorption complexes of AMP (a), CMP (b), GMP (c), and UMP (d): $\equiv CeOH_2^+ HL^-$ (*1*) and $\equiv CeOH_2^+ L^{2-}$ (2)

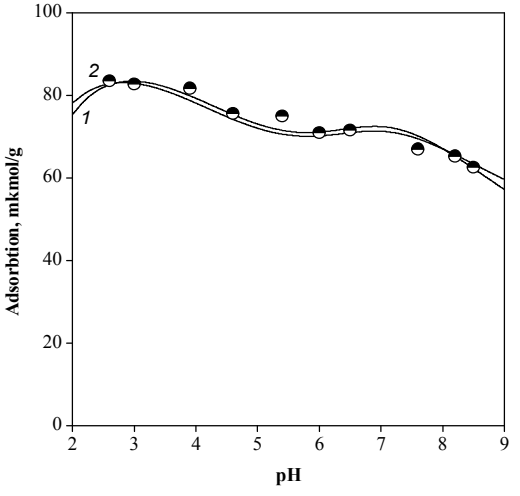

Fig. 6. Adsorption of orthophosphate on the ceria surface as a function of pH: C_{OP} = 0.1 mmol/L, C_{oxide} = 1 g/L, 0.01 M NaCl. Experimental data are represented by symbols, and the adsorption curves calculated on the assumption of the outer sphere (1) and inner sphere (*2*) complex formation are shown as solid lines

$$\equiv CeOH + HO(P{=}O)(OH)_2 \leftrightarrow$$
$$\leftrightarrow \equiv CeO(P{=}O)(OH)O^- + H^+ + H_2O, \quad (3)$$
$$\equiv CeOH + HO(P{=}O)(OH)_2 \leftrightarrow$$
$$\leftrightarrow \equiv CeO(P{=}O)O_2^{2-} + 2H^+ + H_2O, \quad (4)$$

where $HO(P{=}O)(OH)_2$ is the formula of orthophosphoric acid (H_3L) which is used to represent more clearly the reaction with the release of protons and water molecules accompanying the formation of inner-sphere complexes.

The best agreement between experimental and calculated values of orthophosphate adsorption is observed when only reaction (4) is taken into account: the stability constant of this complex is $\log K^{int}_{CeOL} = 7.40 \pm 0.05$. A positively charged surface promotes the formation of a negatively charged complex, while the inner sphere complex formed through reaction (2) would be electrically neutral. It is not clear why a complex with a singly charged phosphate anion is not formed in this case, but nevertheless, the stability of such a complex and its share in the total adsorption value is insignificant. It can be seen from Fig. 6 that the adsorption curves calculated on the assumption of outer and inner-sphere complexes formation practically coincide. Assuming that in nucleotide surface complexes phosphate anions are bound with functional groups, we tried to simulate the adsorption as inner-sphere complex formation. The best agreement between the experimental and calculated adsorption curves is observed when we assume the formation of only one complex $\equiv CeOL^-$ according to the reaction:

$$\equiv CeOH + HO(P{=}O)(OR)O^- \leftrightarrow$$
$$\leftrightarrow \equiv CeO(P{=}O)(OR)O^- + H_2O,$$

where $HO(P{=}O)(OR)O^-$ is a monoanion of nucleotide (R – nucleoside residue).

The calculated stability constants of inner sphere nucleotide complexes are represented in Table 2 (reaction 7). As in the case of the outer sphere complex formation, more stable complexes are formed by AMP, CMP, and GMP. Fig. 7 shows the structures of nucleotide complexes adsorbed on the surface of cerium dioxide.

We consider all inner-sphere complexes as monodentate ones; it was suggested that one of the hydroxyl groups of phosphate anion reacts with one functional group of the oxide. At the same time complexes with different structures, at least for phosphate, are available in the literature.[36-38,40,41] These structures include bridging bidentate complexes, in which two OH groups of phosphate react with two neighboring ≡MOH groups, and chelate complexes, which are formed via the interaction of two OH groups of phosphate with two OH groups of one metal atom. The formation of the monodentate inner-sphere complex was confirmed in the study of nucleotides adsorption on the surface of alumina.[42] In our opinion, there is currently no sufficient evidence of the formation of complexes with a certain structure. Moreover, this can be assumed for complex aggregates such as nucleotide surface complexes, which are more sophisticated ones than those formed by inorganic phosphates. Establishing the exact structure of such complexes requires careful study using appropriate spectroscopic methods.

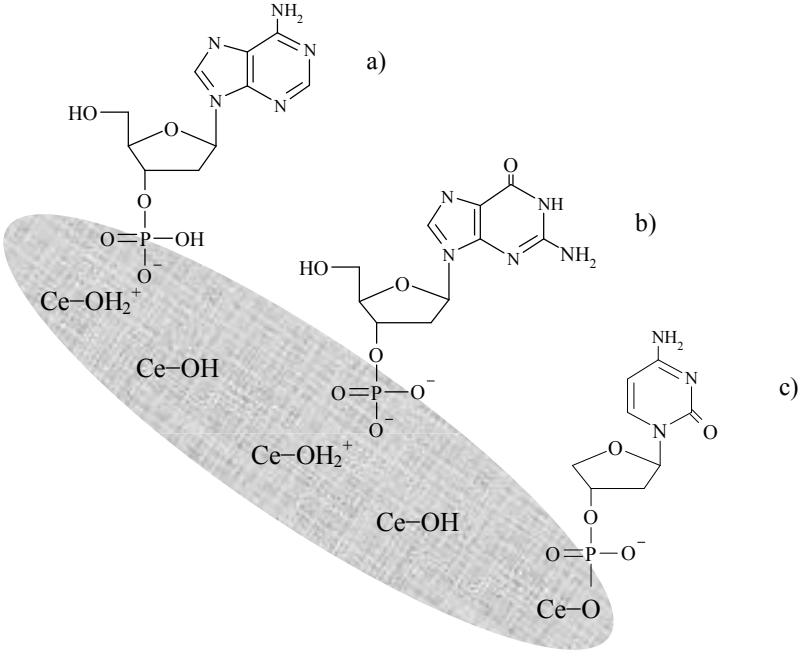

Fig. 7. A schematic of nucleotide surface complexes: outer sphere electrostatic complexes with singly charged anion (a), doubly charged anion (b), and inner sphere covalent complex (c)

4. Conclusions

Thus, it has been shown that the adsorption of nucleotides on a cerium dioxide surface may be represented and quantitatively characterized as a formation of outer and inner-sphere complexes due to electrostatic and covalent interactions. Electrostatic attraction of differently charged particles promotes the approach of nucleotide molecules to such a distance from the surface that covalent interactions become possible. The involvement of phosphate groups in binding to the oxide surface suggests that nucleic acids interact with the surface of inorganic oxide materials similar to the nucleotides of which they are composed. Our results provide a better understanding of nano-biointeraction between natural polymers and oxides.

References

[1] Nel, A.E.; Madler, L.; Velegol, D.; Xia, T.; Hoek, E.M.V.; Somasundaran, P.; Klaessig, F.; Vince Castranova, V.; Thompson, M. Understanding Biophysicochemical Interactions at the Nano–Bio Interface. *Nat. Mater*. **2009**, *8*, 543-557. https://doi.org/10.1038/nmat2442

[2] Vallee, A.; Humblot, V.; Pradier, C.-M. Peptide Interactions with Metal and Oxide Surfaces. *Acc. Chem. Res*. **2010**, *43* (10), 1297-1306. https://doi.org/10.1021/ar100017n

[3] Stark, W.J. Nanoparticles in Biological Systems. *Angew. Chem. Int. Ed.* **2011**, *50* (6), 1242-1258. https://doi.org/10.1002/anie.200906684

[4] Shemetov, A.; Nabiev, I.; Sukhanova, A. Molecular Interaction of Proteins and Peptides with Nanoparticles. *ACS Nano* **2012**, *6* (6), 4585-4602. https://doi.org/10.1021/nn300415x

[5] Huang, R.; Lau, B.L.T. Biomolecule–Nanoparticle Interactions: Elucidation of the Thermodynamics by Isothermal Titration Calorimetry. *Biochim. Biophys. Acta Gen. Subj.* **2016**, *1860* (5), 945-956. https://doi.org/10.1016/j.bbagen.2016.01.027

[6] Gunnarsson, S.B.; Bernfur, K.; Mikkelsen, A.; Cedervall, T. Analysis of Nanoparticle Biomolecule Complexes. *Nanoscale* **2018**, *10*, 4246-4257. https://doi.org/10.1039/c7nr08696b

[7] Xu, C.; Qu, X. Cerium Oxide Nanoparticle: A Remarkably Versatile Rare Earth Nanomaterial for Biological Applications. *NPG Asia Mater*. **2014**, *6*, e90. https://doi.org/10.1038/am.2013.88

[8] Shcherbakov, A.B.; Zholobak, N.M.; Ivanov, V.K. Biological, Biomedical and Pharmaceutical Applications of Cerium Oxide. In *Cerium Oxide (CeO_2): Synthesis, Properties and Applications*; Scire, S.; Palmisano L., Eds.; Elsevier, 2019; pp 279-358.

[9] Asati, A.; Santra, S.; Kaittanis, C.; Nath, S.; Perez, J.M. Oxidase-Like Activity of Polymer-Coated Cerium Oxide Nanoparticles. *Angew. Chem Int. Ed*. **2009**, *121*, 2344-2348. https://doi.org/10.1002/ange.200805279

[10] Li, X.; Sun, L.; Ge, A.; Guo, Y. Enhanced Chemiluminescence Detection of Thrombin Based on Cerium Oxide Nanoparticles. *Chem. Comm.* **2011**, *47*, 947-949. https://doi.org/10.1039/C0CC03750H

[11] Kaittanis, C.; Santra, S.; Asati, A.; Perez, J.M. A Cerium Oxide Nanoparticle-Based Device for the Detection of Chronic Inflammation *via* Optical and Magnetic Resonance Imaging. *Nanoscale* **2012**, *4*, 2117-2123. https://doi.org/10.1039/C2NR11956K

[12] Ornatska, M.; Sharpe, E.; Andreescu, D.; Andreescu, S. Paper Bioassay Based on Ceria Nanoparticles as Colorimetric Probes. *Anal. Chem*. **2011**, *83* (11), 4273-4280. https://doi.org/10.1021/ac200697y

[13] Xu, C.; Lin, Y.; Wang, J.; Wu, L.; Wei, W.; Ren, J.; Qu, X. Nanoceria-Triggered Synergetic Drug Release Based on CeO_2-Capped Mesoporous Silica Host–Guest Interactions and Switchable Enzymatic Activity and Cellular Effects of CeO_2. *Adv. Healthc. Mater*. **2013**, *2* (12), 1591-1599. https://doi.org/10.1002/adhm.201200464

[14] Li, M.; Shi, P.; Xu, C.; Ren, J.; Qu, X. Cerium Oxide Caged Metal Chelator: Anti-Aggregation and Anti-Oxidation Integrated H_2O_2-Responsive Controlled Drug Release for Potential Alzheimer's Disease Treatment. *Chem. Sci*. **2013**, *4*, 2536-2542. https://doi.org/10.1039/C3SC50697E

[15] Karakoti, A. S.; Tsigkou, O.; Yue, S.; Lee, P.D.; Stevens, M.M.; Jones, J.R.; Seal, S. Rare Earth Oxides as Nanoadditives in 3-D Nanocomposite Scaffolds for Bone Regeneration. *J. Mater. Chem*. **2010**, *20*, 8912-8919. https://doi.org/10.1039/C0JM01072C

[16] Mandoli, C.; Pagliari, F.; Pagliari, S.; Forte, G.; Di Nardo, P.; Licoccia, S.; Traversa, E. Stem Cell Aligned Growth Induced by CeO_2 Nanoparticles in PLGA Scaffolds with Improved Bioactivity for Regenerative Medicine. *Adv. Funct. Mater*. **2010**, *20* (10), 1617-1624. https://doi.org/10.1002/adfm.200902363

[17] Pautler, R.; Kelly, E.Y.; Huang, P.-J. J.; Cao, J.; Liu, B.; Liu, J. Attaching DNA to Nanoceria: Regulating Oxidase Activity and Fluorescence Quenching. *ACS Appl. Mater. Interfaces* **2013**, *5* (15), 6820-6825. https://doi.org/10.1021/am4018863

[18] Liu, B.; Sun, Z.; Huang, P.-J.J.; Liu, J. Hydrogen Peroxide Displacing DNA from Nanoceria: Mechanism and Detection of Glucose in Serum. *J. Am. Chem. Soc*. **2015**, *137* (3), 1290-1295. https://doi.org/10.1021/ja511444e

[19] Huang, C.-J.; Lin, Z.-E.; Yang, Y.-S.; Chan, H.W.-H.; Chen, W.-Y. Neutralized Chimeric DNA Probe for Detection of Single Nucleotide Polymorphism on Surface Plasmon Resonance Biosensor. *Biosens. Bioelectron*. **2018**, *99*, 170-175. https://doi.org/10.1016/j.bios/2017.07.052

[20] Liu, B.; Liu, J. Accelerating Peroxidase Mimicking Nanozymes Using DNA. *Nanoscale* **2015**, *7*, 13831-13835. https://doi.org/10.1039/C5NR04176G

[21] Thurn, K.T.; Paunescu, T.; Wu, A.; Brown, E.M.B.; Lai, B.; Vogt, S.; Maser, J.; Aslam, M.; Dravid, V.; Bergan, R. *et al.* Labeling TiO_2 Nanoparticles with Dyes for Optical Fluorescence Microscopy and Determination of TiO_2–DNA Nanoconjugate Stability. *Small* **2009**, *5* (11), 1318-1325. https://doi.org/10.1002/smll.200801458

[22] Bülbül, G.; Hayat, A.; Andreescu, S. ssDNA-Functionalized Nanoceria: A Redox-Active Aptaswitch for Biomolecular Recognition. *Adv. Healthc. Mater*. **2016**, *5* (7), 822-828. https://doi.org/10.1002/adhm.201500705

[23] Kim, M.I.; Park, K.S.; Park, H.G. Ultrafast Colorimetric Detection of Nucleic Acids Based on the Inhibition of the Oxidase Activity of Cerium Oxide Nanoparticles. *Chem. Comm.* **2014**, *50*, 9577-9580. https://doi.org/10.1039/C4CC03841J

[24] Costa, D.; Garrain, P.-A.; Baaden, M. Understanding Small Biomolecule-Biomaterial Interactions: A Review of Fundamental Theoretical and Experimental Approaches for Biomolecule Interactions with Inorganic Surfaces. *J. Biomed. Mater. Res. A*., **2013**, *101A* (4)**,** 1210-1222. https://doi.org/10.1002/jbm.a.34416

[25] Westall, J.C.; Hohl, H. A Comparison of Electrostatic Models for the Oxide/Solution Interface. *Adv. Colloid Interface Sci*. **1980**, *12* (4), 265-294. https://doi.org/10.1016/0001-8686(80)80012-1

[26] Cristl, I.; Kretzschmar ,R. Competitive Sorption of Copper and Lead at the Oxide-Water Interface: Implications for Surface Site Density. *Geochim. Cosmochim. Acta* **1999**, *63* (19-20), 2929-2938. https://doi.org/10.1016/S0016-7037(99)00266-5
[27] Ludwig, Chr. *GRFIT, a Program for Solving Speciation Problems, Evaluation of Equilibrium Constants, Concentrations, and Other Physical Parameters*; Internal Report of University of Bern, 1992.
[28] Davis, J.A.; Kent D.B. Surface Complexation Modeling in Aqueous Geochemistry. In *Mineral-Water Interface Geochemistry*; Hochella, M.F,; White, A.F., Eds.; California, USA., 1990; pp 177-260. https://doi.org/10.1515/9781501509131
[29] Kosmulski, M. *Chemical Properties of Materials Surfaces*; Marcel Dekker: New York – Basel, 2001.
[30] Saenger, W. *Principles of Nucleic Acid Structure*; Springer: New York, 1984.
[31] Smith, R.M.; Martell, A.E.; Chen, Y. Critical evaluation of stability constants for nucleotide complexes with protons and metal ions and the accompanying enthalpy changes. *Pure Appl. Chem.* **1991**, *63* (7), 1015-1080. https://doi.org/10.1351/pac199163071015
[32] Thaplyal, P.; Bevilacqua, P.C. Chapter Nine - Experimental Approaches for Measuring pK_a's in RNA and DNA. *Methods Enzymol.* **2014**, *549*, 189-219. https://doi.org/10.1016/B978-0-12-801122-5.00009-X
[33] Childs, C.W. Potentiometric Study of Equilibriums in Aqueous Divalent Metal Orthophosphate Solutions. *Inorg. Chem.* **1970**, *9* (11), 2465-2269. https://doi.org/10.1021/ic50093a017
[34] Galal-Gorchev, H.; Stumm, W.J. The Reaction of Ferric Iron with ortho-Phosphate. *J. Inorg. Nucl. Chem.* **1963**, *25* (5), 567-574. https://doi.org/10.1016/0022-1902(63)80243-2
[35] Martell, A.E.; Smith, R.M. *Critical Stability Constants. V. 4. Inorganic Complexes*; Springer: New York, 1974.
[36] Connor, P.A.; McQuillan, A.J. Phosphate Adsorption onto TiO_2 from Aqueous Solutions: An *in Situ* Internal Reflection Infrared Spectroscopic Study. *Langmuir* **1999**, *15* (8), 2916-2921. https://doi.org/10.1021/la980894p
[37] Michelmore, A.; Gong, W.; Jenkins, P.; Ralston, J. The Interaction of Linear Polyphosphates with Titanium Dioxide Surfaces. *Phys. Chem. Chem. Phys.* **2000**, *2*, 2985-2992. https://doi.org/10.1039/B001213K
[38] Gong, W. A Real Time in Situ ATR-FTIR Spectroscopic Study of Linear Phosphate Adsorption on Titania Surfaces. *Int. J. Miner. Process.* **2001**, *63* (3), 147-164. https://doi.org/10.1016/S0301-7516(01)00045-X
[39] Rahnemaie, R.; Hiemstra, T.; Van Riemsdijk, W.H. Geometry, Charge Distribution, and Surface Speciation of Phosphate on Goethite. *Langmuir* **2007**, *23* (7), 3680-3689. https://doi.org/10.1021/la062965n
[40] Kang, S.A.; Li, W.; Lee, H.E.; Phillips, B.L.; Lee, Y.J. Phosphate Uptake by TiO_2: Batch Studies and NMR Spectroscopic Evidence for Multisite Adsorption. *J. Colloid Interface Sci.* **2011**, *364* (2), 455-461. https://doi.org/10.1016/j.jcis2011.07.088
[41] Tielens, F.; Gervais, C.; Deroy, G.; Jaber, M.; Stievano, L.; Diogo, C.C.; Lambert, J.-F. Characterization of Phosphate Species on Hydrated Anatase TiO_2 Surfaces. *Langmuir* **2016**, *32* (4), 997-1008. https://doi.org/10.1021/acs.langmuir.5b03519
[42] Feuillie, C.; Sverjensky, D.A.; Hazen, R.M. Attachment of Ribonucleotides on α-Alumina as a Function of pH, Ionic Strength, and Surface Loading. *Langmuir* **2015**, *31* (1), 240-248. https://doi.org/10.1021/la504034k

Received: September 08, 2021 / Revised: September 26, 2021 / Accepted: October 04, 2021

ВЗАЄМОДІЯ НУКЛЕОТИДІВ З ПОВЕРХНЕЮ НАНОКРИСТАЛІЧНОГО ДІОКСИДУ ЦЕРІЮ

Анотація. *Було досліджено адсорбцію нуклеотидів на поверхні нанокристалічного діоксиду церію ($pH_{ТНЗ}$ = 6,3) з водних розчинів NaCl у широкому діапазоні pH. Одержані результати було інтерпретовано як утворення зовнішньо- та внутрішньосферних комплексів за участі фосфатних залишків. Для кількісного визначення констант рівноваги реакцій було застосовано базову модель комплексоутворення на поверхні Штерна.*

Ключові слова: *діоксид церію, нуклеотид, адсорбція, теорія комплексоутворення на поверхні.*